

# Numerical estimation of discharge probability in GEM-based detectors

---

**Prasant Kumar Rout,<sup>a,b,1</sup> R. Kanishka,<sup>a,b</sup> Jaydeep Datta,<sup>a,b</sup> Promita Roy,<sup>a,b</sup> Purba Bhattacharya,<sup>c</sup> Supratik Mukhopadhyay,<sup>a,b</sup> Nayana Majumdar,<sup>a,b</sup> Sandip Sarkar<sup>a,b</sup>**

<sup>a</sup>*Saha Institute Of Nuclear Physics,  
1/AF Saltlake, Kolkata 700064, India*

<sup>b</sup>*Homi Bhabha National Institute, Training School Complex,  
Anushaktinagar, Mumbai 400094, India*

<sup>c</sup>*Department of Physics, University of Calcutta,  
92 A.P.C Road, Kolkata 700009, West Bengal, India*

E-mail: [prasantrout7@gmail.com](mailto:prasantrout7@gmail.com)

**ABSTRACT:** Discharge probability in GEM-based gaseous detectors has been numerically estimated using an axisymmetric hydrodynamic model. Initial primary charge configurations in the drift region, obtained using Heed and Geant4, are found to have significant effect on the subsequent evolution of detector response. Simulation of energy resolution has been performed to establish the capability of the hydrodynamic model to capture statistical nature of the experimental situation. Finally, single and triple GEM configurations exposed to alpha sources have been simulated to estimate discharge probability which have been compared with available experimental data. Despite the simplifying and drastic assumptions in the numerical model, the comparisons are encouraging.

**KEYWORDS:** Detector modelling and simulations II, Micropattern gaseous detectors (GEM), Electron multipliers (gas), Gaseous detectors, Charge transport and multiplication in gas, Avalanche-induced secondary effects

ARXIV EPRINT: [1234.56789](https://arxiv.org/abs/2103.12849)

---

<sup>1</sup>Corresponding author.

---

## Contents

<b>1</b>	<b>Introduction</b>	<b>1</b>
<b>2</b>	<b>Simulation details</b>	<b>3</b>
2.1	Generation of primaries	3
2.2	Transport and amplification of primaries	4
<b>3</b>	<b>Results and Discussions</b>	<b>5</b>
3.1	Energy resolution estimate	5
3.2	Primary ionization	6
3.3	Method of estimating discharge probability	8
3.4	Discharge probability estimates	9
<b>4</b>	<b>Conclusion</b>	<b>13</b>

---

## 1 Introduction

Micro-Pattern Gaseous Detectors, in particular the Gas Electron Multiplier(GEM) [1], are widely used in the high luminosity experiments such as COMPASS [2], LHCb [3], ALICE [4], CMS [5] and TOTEM [6, 7]. Over the years a lot of effort has been put together in the research and development of this technology for improving the performance of GEM-based detectors for long term operation in the mentioned high rate experiments. These detectors have been used both as tracking and triggering detectors due to their excellent spatial resolution of  $\sim 30 \mu m$  and time resolution in the nanosecond range [8]. Apart from the position and time resolution performances of these detectors, parameters like radiation hardness, aging resistance, high rate capability and high voltage stability against electrical discharges are of crucial importance, especially for long term operation of different experiments. Electrical discharges are among the most important threats to all the experiments that may lead to instability and irreversible damages to the detectors. As a result, many studies have been performed to investigate formation of discharge in GEM-based detectors [9–12].

There are several factors that determine the transition from avalanche to streamer formation. Some of the more prominent ones are the number of primaries, electric field configuration and the transport, amplification, attachment properties of the gas mixture. There is general agreement that the transition from avalanche to streamer is dependent on a critical charge density, termed as the Raether limit [13]. This limit is found to be dependent on the gas mixture and is reported to be within the range  $(5-9) \times 10^6$  [14] for Argon(Ar)-based and Neon(Ne)-based mixtures. Large charge densities produced in the drift region by highly-ionizing particles like alpha makes the detector prone to streamers and hence significantly alter the stability of the detector. It has also been observed in [14] that if the charge deposit occurs close to the GEM hole, discharge probability is higher. The use of highly-ionizing alpha source on single, double and triple GEM detectors with

Ar-based gas mixtures was also reported in [15]. The relation of discharge probability with number of primaries in the drift region indicates that these detectors are likely to face increasing difficulty as the luminosity of the experiments increase.

In multistage GEM-based detectors, the gas amplification process is shared among the GEM foils and this can be used to delay the onset of streamers in such configurations. According to [16], the occurrence of discharge can be prevented by decreasing the gas amplification from top to bottom foils towards the end of the anode so that it does not reach the critical avalanche size. This is possible by lowering the applied potential difference across different GEMs successively from top to bottom foils. This lowering scheme of potential difference across GEM foils has been experimentally illustrated in [15] and such an asymmetric distribution of potential differences was successfully used in COMPASS [17, 18]. Recently, the triple GEM detectors being used to upgrade the Muon system of CMS [5] also implements similar distribution of amplification fields in different GEM layers. This distribution, however, has adverse effect on the ion back-flow suppression which is of importance for a GEM-based TPC [19–21].

Computer simulation of streamers is known to be a difficult problem because of the strongly nonlinear nature of the phenomenon. While several attempts have been made in different contexts [22–25], as far as we know, only few attempts have been made to model discharges in gaseous ionization detectors, despite its acknowledged importance in various experimental situations [14]. As a result, estimation of discharge probability using purely numerical approach has remained beyond the reach of the detector community. In [14], in addition to experimental studies, a numerical model based on Geant4 has been used to estimate the discharge probability for single GEMs with success. However, aspects related to the transport and amplification were ignored in the model and a combination of computational and experimental approach was utilized instead. Moreover, a discharge was defined by comparing the number of accumulated charges inside a single GEM hole with a predefined critical charge limit that was estimated separately. The dynamics of processes leading to the charge accumulation was not followed in detail and the transition from avalanche to streamer was not simulated. It is easy to appreciate that a relatively more independent and reliable numerical estimation of discharge probability will be of significant help to different experimental groups, especially if it can be used to analyze multi-GEM detectors as well. In this work, attempts have been made to address this issue by developing a hybrid numerical model to simulate the entire chain of events starting from primary ionization to formation of avalanche, or streamers in single and triple GEM detectors. Attempts have been made to estimate discharge probability in such detectors being operated under different experimental conditions using the same numerical model.

The proposed model is based on a recently-developed hydrodynamic model [26] which could simulate the transition from avalanche to streamers in multiple GEM-based detectors reasonably well. It was found, in agreement with several earlier numerical models [14, 27–29], that the presence of high charge densities in the close vicinity of GEM foil gives rise to the space charge dominated positive streamers in GEM detectors. In the present paper, we have extended the 2D axisymmetric hydrodynamic model to simulate the response of single and triple GEM detectors exposed to different radiation sources, as well as to estimate discharge probabilities due to heavily-ionizing alpha particles. The simulated results are obtained with the Ar–Carbon dioxide( $\text{CO}_2$ ) gas mixture in volume proportions 70–30. In order to emulate the statistical nature of different processes

determining the evolution of charge transport within the detector, fluctuations in primary electron configurations have been considered in fair detail. The rest of the present paper is organized as follows. Section 2 describes numerical model adopted for estimating the primary ionization following which the transport and amplification of charges in the gas volume is discussed. The details of the hydrodynamic model were described in detail in [26] and are briefly mentioned here. Section 3 contains energy resolution estimates that is used to establish the capability of the proposed model to reproduce statistical processes. The method adopted for estimating discharge probability and the simulated values of the discharge probability are also presented in this section and compared with experimental results from [15]. Finally, section 4 contains the summary of the work and few concluding remarks.

## 2 Simulation details

The numerical studies have been carried out in two steps: (1) Generation of primaries, (2) Transport and amplification of primaries. The first step is carried out using Monte Carlo models, while the latter uses a hydrodynamic model, resulting into a hybrid numerical model for the entire process. Here, both the numerical steps are described in brief.

### 2.1 Generation of primaries

This initial distribution of primary electrons plays an important role in determining the subsequent evolution of the charged particles. Estimation of such initial configurations is conveniently implemented using Monte-Carlo techniques. Thus, in this part of the computation, number and location of primaries generated within the detector gas volume are estimated using Geant4 [30] and Heed [31], depending on the type of source used. For example, the former was used to estimate the primaries generated due to an alpha source, as described in some detail below.

In the experimental arrangement described in [15], a collimated beam of alpha particles with an angular opening of  $\pm 30^\circ$  from an  $^{241}\text{Am}$  alpha source placed on a thin ( $3.5\ \mu\text{m}$ ) mylar window external to the semi transparent drift cathode was used for measurement of discharge probability. Following this description, a three-dimensional simulation geometry has been created in Geant4, that closely mimics the experimental arrangement. A collimated beam of alpha particles with an angular opening of  $\pm 30^\circ$  passing through a thin mylar window of thickness  $3.5\ \mu\text{m}$  has been injected into the gas volume of the numerical model. This active gas volume, made up of  $\text{Ar-CO}_2$  in proportions 70–30 by volume, was considered to be a three-dimensional box of dimensions 5 cm along x, 5 cm along y and 20 cm along z direction. Geant4 follows particle transport in prefixed, or automatically decided steps with possibility of an interaction after each step. The step-lengths are computed according to the cross-sections of physics processes to be considered for a particular simulation. The possible physics processes are maintained in different physics lists among which the user selects a few depending on their suitability for simulating a given physics problem. For the present studies, physics lists like EmPenelope, EmLivermorePhysics, Photo Absorption Ionization (PAI) and PAI-photon were used to simulate the particle interactions with the active detector material. The position and energy deposit of each individual GEANT4 hit were extracted from the simulation for each of the alpha tracks in the gas volume. Results corresponding to such event generation exercises will be presented in section 3.2.

## 2.2 Transport and amplification of primaries

Processes subsequent to the generation of primaries, namely, drift, diffusion, amplification, attachment, etc. have been simulated using a 2D axisymmetric hydrodynamic model of GEM detectors, as described in detail in [26]. According to this model, transport, Townsend amplification, photon feedback and attachment of charged fluid in the presence of externally applied electric field lead to formation of avalanche and streamer in the detector volume. One of the major advantages of this approach is the natural inclusion of space charge effects throughout the evolution of the charged species. The stopping conditions described in [26] have been used to identify avalanche and streamer events. The 2D axisymmetric model of single and triple GEM configurations are shown in figures 1 (a) and (b), respectively. The electric field configuration and the parameters of the detector geometries follow the description of [15] and are shown in table 1.

GEM Structures	Range $\Delta V_{\text{GEM}}(\text{V})$	Drift Field (kV/cm)	Transfer Field (kV/cm)	Induction Field (kV/cm)	Gap (mm)
Single GEM	500 - 515	2	-	3.5	3:1
Triple GEM	385 - 400	2	3.5	3.5	3:1:1:1

**Table 1.** Electric potential, field configuration and geometrical parameters for single and triple GEM structures used in the simulation

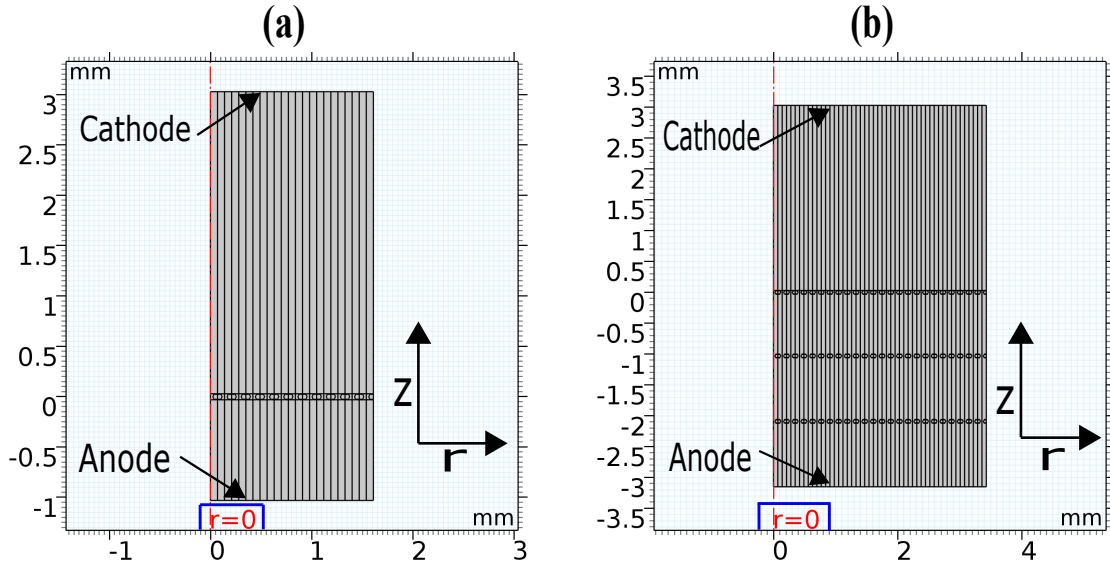


**Figure 1.** 2D axisymmetric geometry of (a) single GEM and (b) triple GEM configurations

One important point to note is the fact that hydrodynamic models are deterministic and influence of statistical fluctuations are usually not implemented when adopting such an approach. However, discharge probability and many other important properties of gaseous ionization detectors are, by nature, statistical and it is important to incorporate this aspect into the final estimates of the numerical model. This has been a major challenge throughout this investigation and, in order to satisfy this requirement, fluctuations arising in primary generation were used as inputs to different executions

of the hydrodynamic model and the final estimate of the statistical quantities were derived from individual results of each of these simulations. It should be mentioned here that the execution time for each of the single GEM configuration for avalanche (streamer) mode operations are around 15 (90) minutes, while for a triple GEM configuration, it was close to 45 (210) minutes respectively, on a Xeon-based workstation having eight cores and 64GB RAM. According to several test executions, the time taken is similar on generation 7 i5 desktop machine having 8GB RAM. In order to confirm that the proposed hybrid numerical model works with dependable accuracy, energy resolutions of single and triple GEM detectors have been estimated and will be presented next in section 3.1.

### 3 Results and Discussions

#### 3.1 Energy resolution estimate

The energy resolution of GEM-based detectors depends on several important factors that include the statistical nature of primary ionization, fluctuations in the gas amplification processes, changes in temperature and pressure, asymmetry in the detector geometry, intrinsic noise in the readout electronics and many more [32]. As a result, the mean energy( $E$ ) of the photon is found to be smeared to a gaussian of standard deviation ( $\sigma_E$ ) instead of a sharp delta function peak and the resolution can be obtained [32] as shown in equations 3.1-3.2.

$$\frac{\sigma_E}{E} = \sqrt{\frac{F}{\bar{n}} + \left(\frac{\sigma_{\bar{G}}}{\bar{G}}\right)^2 + (\Delta_0^2)} \quad (3.1)$$

$$\frac{\Delta E_{FWHM}}{E} = 2\sqrt{\ln 4} \frac{\sigma_E}{E} \approx 2.355 \frac{\sigma_E}{E} \quad (3.2)$$

Here,  $F$  is the gas-dependent Fano factor and its value for Ar has been considered to be  $\sim 0.23$  [32].  $\bar{G}$  is the mean gas gain,  $\sigma_{\bar{G}}$  being the standard deviation of  $\bar{G}$ . The quantity  $\bar{n}$  represents the average number of primaries found to be 211 using [31] and  $\Delta_0$  represents the effects of fluctuations like foil asymmetry, temperature and pressure, etc. The energy resolution has been expressed as Full Width Half Maximum (FWHM) over the mean energy  $E$  in equation 3.2.

The energy resolution of a single GEM detector in response to 5.9 keV photon from  $^{55}\text{Fe}$  radiation source has been estimated. In the proposed hybrid numerical model, the variation of gain has been modelled by changing the position and cluster spread of the seed cluster in the drift gap. Realistic configurations of the seed clusters have been set up by analysing the number and location information of the primaries as obtained using [31]. In the present version of the model,  $\Delta_0$  has been considered to be zero.

The numerical estimates of gas gain were presented in [26] for single, double and triple GEM detectors using the  $^{55}\text{Fe}$  radiation source. The estimates were obtained considering mean cluster spread of 0.132 mm and 0.154 mm along  $r$  and  $z$  direction, while the cluster was considered to be located at 0.250 mm above the top GEM foil. Following figure 4 of [26], the gaussian fitted  $\pm 1\sigma$  variation from the mean cluster spread along  $r$  (0.071 mm) and  $z$  (0.08 mm) directions has been chosen in the present study. In addition to the mean cluster spread, other four extreme cases of cluster configuration have been obtained by addition and subtraction of  $1\sigma$  from the mean cluster spread in  $r$  and  $z$  directions in the present study and are shown in table 2. Evolution of the charged

species was studied using the mentioned hydrodynamic model using each case as the initial seed situated at four z positions, namely 0.250 mm, 0.5 mm, 0.75 mm and 0.9 mm.

The position and shape of seed cluster in the drift gap affect the drift and diffusion of electrons and ions that lead to different charge sharing patterns in the GEM holes. The contribution of the primary electrons to the central hole of an axisymmetric geometry reduces significantly with increasing distance of the primary cluster from the top of the GEM foil. Approximate correction factors for scaling the axisymmetric estimates of the gain to that of 3D gain values have been derived for different configurations of the primary charge cluster, following the description of [26]. Figure 2(a) shows the numerical estimates of effective gain with the mean z position of the primary cluster for a single GEM with  $\Delta V_{GEM} = 470$  V. The variation of effective gain with voltages applied to a single GEM detector for different shapes of the primary cluster placed at a certain position ( $z = 0.9$  mm) in the drift gap has also been shown in figure 2(b). Similarly, effective gain of a triple GEM detector for a fixed  $\Delta V_{GEM} = 350$  V applied to the three GEM foils with different z positions of the seed cluster in the drift gap has been shown in figure 2(c), while variation of gain with applied voltages to the three GEM foils of a triple GEM is shown in figure 2(d). It may be noted that both position and shape of the primary cluster have significant effect on the estimated effective gain. From these plots, it is observed that the enlarged (case 2) and r-elongated (case 4) seeds tend to result into larger values of gain. The rest of the configurations, namely, mean, shrunk and z-elongated, give rise to similar values of gains. Moreover, seeds located at larger distances from the GEM top lead to larger values of gain.

The energy resolutions for single and triple GEM detectors have been estimated considering the fact that all possible cases of primary cluster variations mentioned above are likely to happen in a real experiment. Figures 2(e) and (f) show the variation of energy resolution with different voltages applied to the GEM foil and effective gain for single and triple GEM detector respectively. Close to 35% of energy resolution has been estimated from the triple GEM detector, whereas, the single GEM energy resolution is estimated to be  $\sim 25\%$ . Similar values of energy resolution for single GEM detector have been reported in [33]. The variation of energy resolution in triple GEM detector is similar to the experimentally observed values reported in [34, 35].

Number of Cases	Description	Cluster spread in r (mm)	Cluster spread in z (mm)
Case 1	mean	0.132	0.154
Case 2	enlarged	0.203	0.234
Case 3	shrunk	0.061	0.074
Case 4	r-elongated	0.203	0.074
Case 5	z-elongated	0.061	0.234

**Table 2.** Five cases of cluster spread for  $^{55}\text{Fe}$  radiation source

### 3.2 Primary ionization

From the brief study in the preceding subsection, it is concluded that the proposed model is capable of estimating statistically fluctuating properties of GEM-based detectors to a reasonable accuracy.



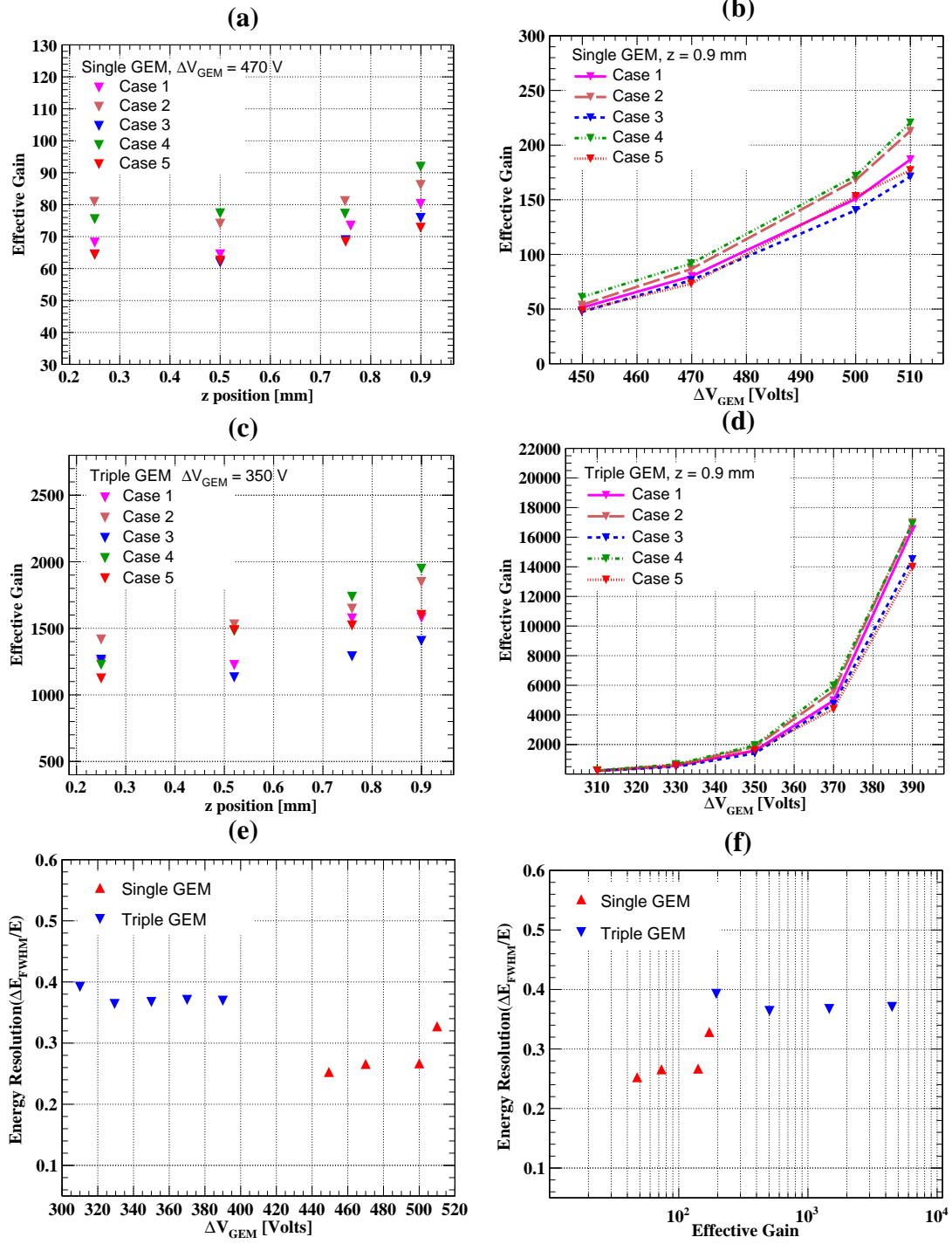


**Figure 2.** (a) Numerical estimates of effective gain variation with different mean  $z$  positions of the primary cluster in a single GEM for five cases of cluster spread at  $\Delta V_{GEM} = 470$  V. (b) Effective gain with different applied voltages to the GEM foils for five different cases of seed cluster spread placed at  $z = 0.9$  mm in the drift gap of single GEM. (c) Effective gain variation with different mean  $z$  positions of primary cluster for five different cases at  $\Delta V_{GEM} = 350$  V. (d) Effective gain with different applied voltages to the GEM foils in five different configurations of seed cluster placed at  $z = 0.9$  mm in the drift gap for a triple GEM. Variation of energy resolution with (e) different applied voltages to GEM foils and (f) effective gain for single and triple GEM detectors



In the remaining part of section 3, numerical estimate of discharge probability will be presented using an  $^{241}\text{Am}$  radiation source which emits 5.6 MeV alpha particles into the Ar–CO<sub>2</sub> gas mixture in volume proportions 70–30. The simulation has been carried out for single and triple GEM structures under different applied voltages as mentioned in table 1. The choice of geometrical parameters of the detectors and the radiation source used follows the experiment described in [15].

A total of 10000 events have been simulated using the Geant4 model described in section 2.1. Tracks resulting from several alpha events, as simulated by the model, have been shown in figure 3(a). For each event, an alpha particle deposits more energy towards the end of the trajectory in the gas volume. As a result, the number density of primaries increases near the Bragg peak. The z position of primaries for an event is shown in figure 3(b). It may be noted that the number of primaries generated in this particular event is nearly  $1.6 \times 10^5$  which is close to the expected value obtained by dividing the energy of the alpha beam by the effective ionization potential of the gas mixture [14]. The range of an alpha particle along the z direction is nearly 4 cm in the gas volume as shown in figure 3(b) which is also reasonably close to the value mentioned in [14]. The differences among the values reported in [14] and the present work are possibly due to differences in simulation details, including the absence / presence of collimation, mylar sheet etc.

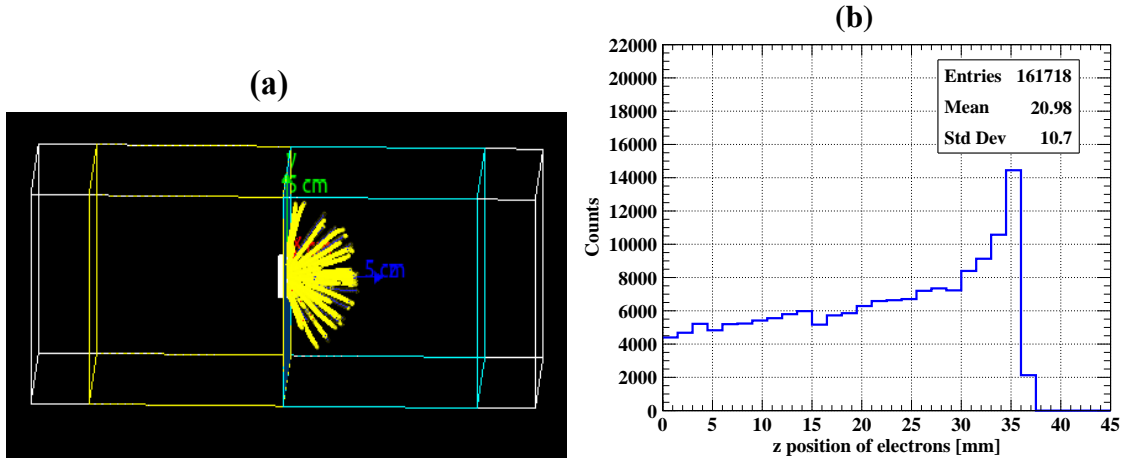


**Figure 3.** (a) Geant4 display of the collimated alpha tracks with an angle of  $\pm 30^\circ$  in Ar–CO<sub>2</sub> (70-30) gas volume. (b) Z position of primary electrons in an event

### 3.3 Method of estimating discharge probability

The hydrodynamic simulation has been initiated utilizing information related to the number fluctuation and spatial distribution of the primaries, as obtained from the preceeding section 3.2. According to [15], the alpha source was placed external to the drift electrode, which is 3 mm above the first GEM foil. Thus, it is assumed that the number of primaries generated in the first 3 mm (z direction) of the simulated gas volume will correspond to the drift gap in the experiment and will contribute to avalanches, or streamers observed in the experiment. Figure 4(a) shows the distribution of number of primaries in each event within the 3 mm gas gap. The cluster spread for each event has been obtained by subtracting the maximum and the minimum radial positions of the primary electrons and is presented in figure 4(b). It may be noted that the primary electrons are uniformly distributed

over the 3 mm gas gap along the  $z$  direction as shown in figure 3(b). For the axisymmetric model considered in this work, the number of electrons being collected by the central hole determines the evolution of the subsequent transport and amplification of the charged species. Because of different transport processes in the drift region, number of electrons are lost in the Copper surfaces of the GEM foil and significant percentage of electrons enter into non-central holes. According to charge sharing data computed following [36], around 50% of primary electrons are found to enter into the central hole. Thus, for each event, the number of primary electrons contributing to the gas amplification process in the central hole has been considered to be 50% of the number indicated in figure 4(a). Figure 4(c) presents a 2D histogram that relates the number of primary electrons in an event with the amount of cluster spread. The initial seed cluster has been represented by a uniform distribution along  $z$  direction and gaussian distribution along the radial direction of the 2D axisymmetric model. The charged fluid computed at the initial moment of the simulation at  $t = 0$  ns has been shown in the figure 4(d). The volume integral of the primary cluster gives the number of primaries present in the simulation volume at the initiation of the hydrodynamic simulation.

The evolution of the charged species and possibility of achieving either an avalanche or streamer mode operation depend on the number of primaries in the drift volume and corresponding spatial distribution, among other simulation parameters, such as potential configuration of the detector etc. Thus, for a given applied voltage to the GEM foil(s), the evolution of the charged fluid has been simulated for several possible combinations of primary electron numbers and cluster spread. Tables 3 and 4 show various combinations of number of primaries and cluster spreads that have been utilized in the simulation for possibility of streamers, with different applied voltages to the GEM foil in single and triple GEM axisymmetric model. According to the present model, clusters of primaries with larger spreads lead to more charge sharing with neighbouring holes and are unlikely to give rise to streamers for a given voltage configuration. Similar observations have also been reported in [15].

### 3.4 Discharge probability estimates

As described in [26], driven by the accumulation of ionic space charge in the central hole, positive streamers are observed in which the charged fluids flow from GEM anode to GEM cathode. The occurrence of such streamers happen in a small fraction of all possible events which include all the possible tracks, as computed by the Geant4 model described earlier in sections 2.1 and 3.2. Finally, in close similarity to definitions used in experimental studies, such as [14], the discharge probability of a given voltage configuration has been defined to be the ratio of the number of possible streamer events estimated by the hydrodynamic model (as indicated in tables 3 and 4) with the total number of possible events estimated from Geant4 simulations.

The resulting streamer probability values have been compared to experimental results presented in [15]. Figures 5(a) and (b) show the discharge probability estimates for single GEM detector with different applied voltages and effective gain and compared with the experimental measurements reproduced from [15]. Similarly, figures 5(c) and (d) show the discharge probability estimates for triple GEM detector with applied voltages and effective gain and compared with the experimental measurements reproduced from [15]. From these figures, it is observed that the discharge probability values in the voltage ranges considered follow the experimental trend for both single and triple GEM

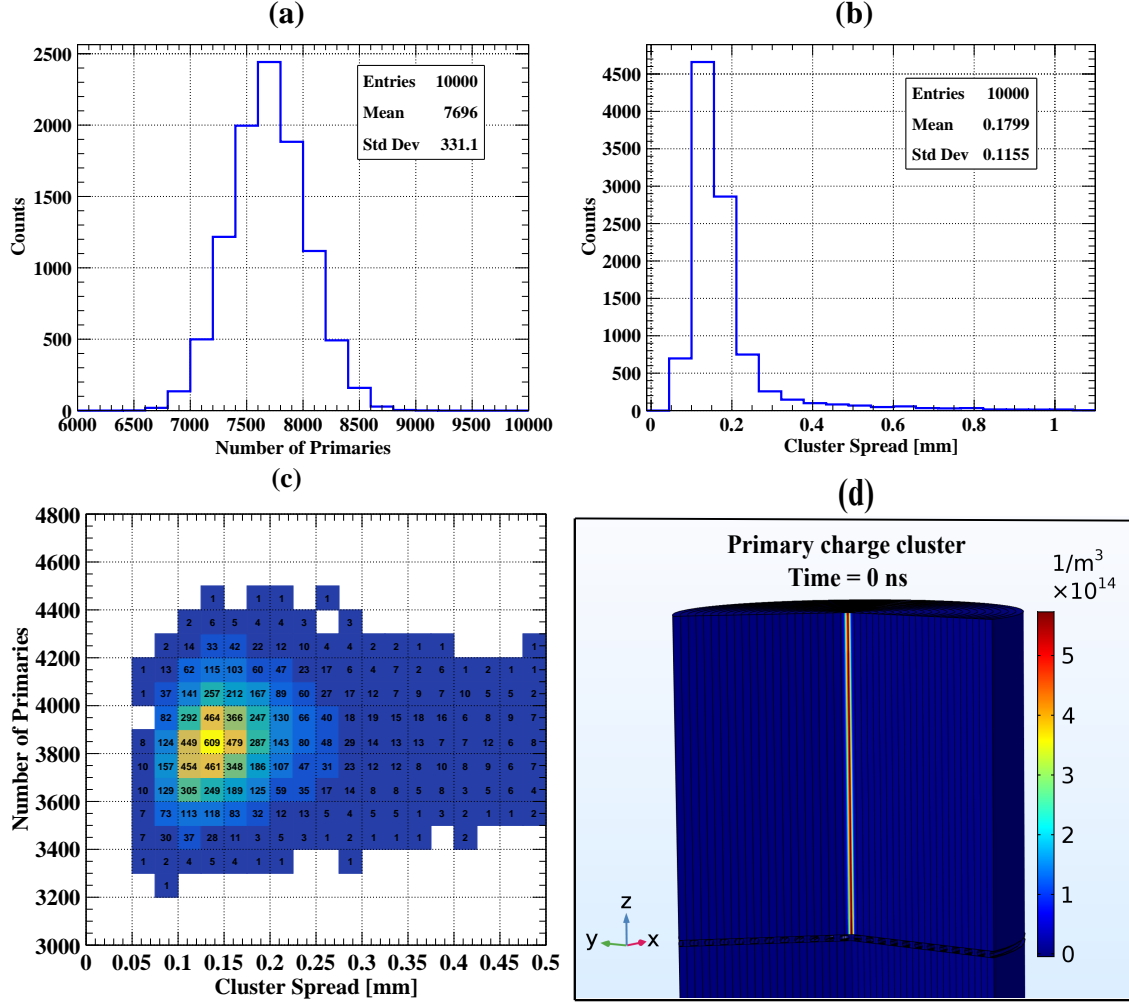


**Figure 4.** (a) Distribution of number of primaries within 3 mm gas gap for 10000 events. (b) Cluster spread distribution in 3mm gas gap for 10000 events. (c) 2D histogram of number of primaries and cluster spread in 3mm gas gap. (d) Primary charge cluster for  $^{241}\text{Am}$  alpha source in the 3 mm drift gap of a single GEM detector at  $t = 0$  ns

detectors. However, the values obtained from the simulation do not exactly match the experimental values, the simulated ones having over-estimated the possibility of streamers.

The simulation has also been performed by applying asymmetric voltages in three GEM foils of the triple GEM detector. A schematic diagram of triple GEM configuration utilized in the simulation for estimating the probability of discharge formation is shown in figure 5 (e). The percentage difference in operating voltages  $[\frac{\Delta V}{V} = \frac{\Delta V_{GEM3} - \Delta V_{GEM1}}{\Delta V_{GEM2}}]$  has been utilized in the simulation and follows closely with the asymmetric configuration (+ 0 -) shown in figure 12 of [15]. The asymmetric configuration (+ 0 -) utilized in simulation represents a fixed voltage of 390 V across GEM2 foil and higher (lower) voltages in GEM1 (GEM3) foils with an equal amount added/subtracted from  $\Delta V_{GEM2}$  respectively. The discharge probability values obtained from simulation are compared with the experimentally observed values reproduced from the asymmetric configuration (+ 0 -) shown in figure 12 of [15]. Figure 5 (f) shows the discharge probability as a function of the

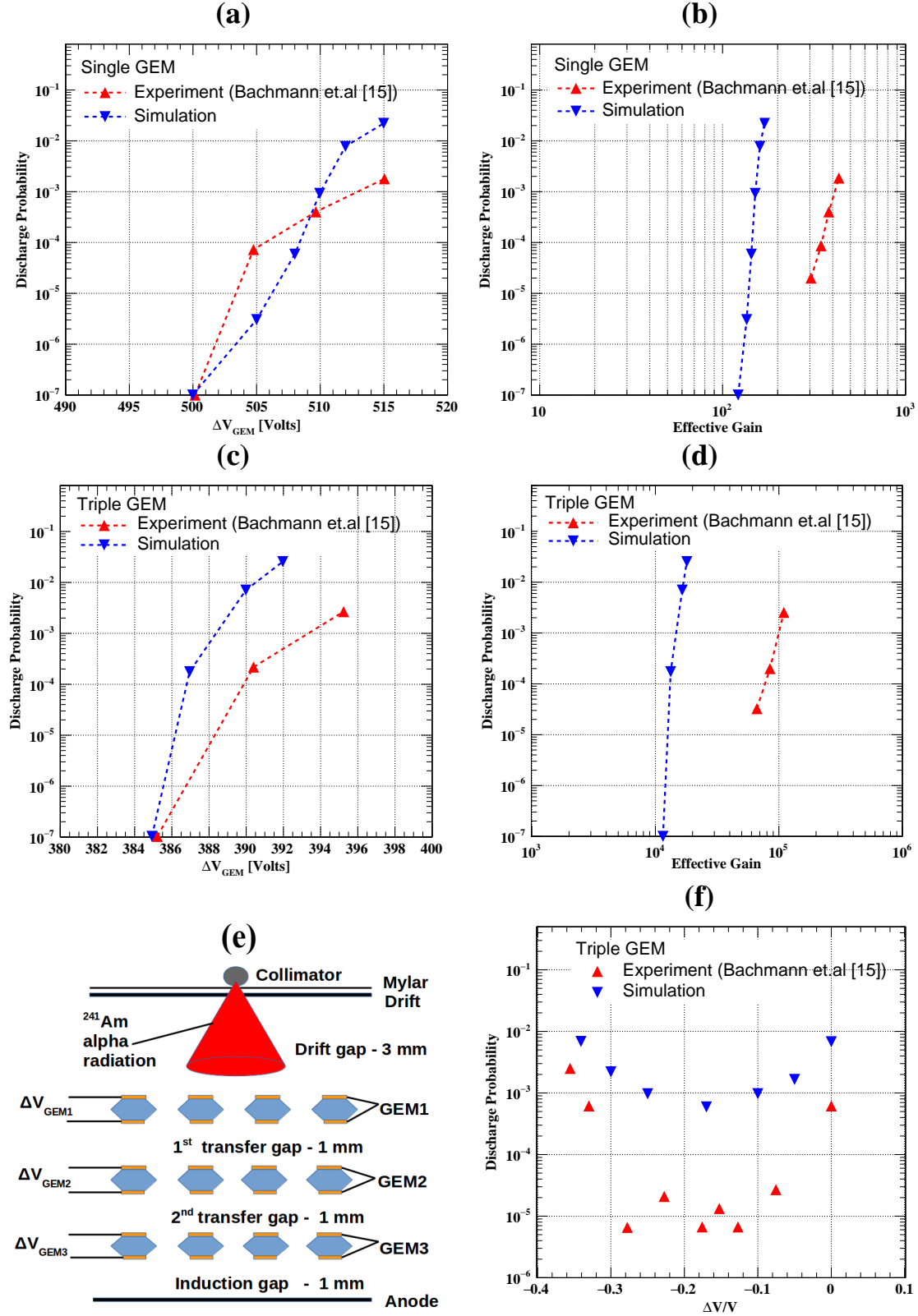


**Figure 5.** Discharge probability estimates in single GEM (a) and (b) obtained from simulation and compared with experimental measurements reproduced from [15]. Discharge probability estimates in triple GEM with equal voltages applied to three GEM foils in (c) and effective gain in (d). (e) Schematic diagram of triple GEM configuration. (f) Discharge probability estimates with asymmetric distribution of voltages obtained from simulation and compared with experimental measurements reproduced from [15].

Applied Voltages $\Delta V_{\text{GEM}}$ (Volts)	Cluster Spread (mm)	Number of Primaries Range	Streamer Yes (No)
500	0.05 - 1.1	All primaries	No
505	0.05 - 1.1	All primaries	No
508	0.050 - 0.085	All primaries	No
	0.085 - 0.125	4300 - 4400 (rest of the primaries)	Yes (No)
	0.125 - 0.175	4400 (rest of the primaries)	Yes (No)
	0.175 - 1.1	All primaries	No
510	0.050 - 0.125	4100 - 4400 (rest of the primaries)	Yes (No)
	0.125 - 0.175	4200 - 4400 (rest of the primaries)	Yes (No)
	0.175 - 1.1	All primaries	No
512	0.050 - 0.125	3800 - 4400 (rest of the primaries)	Yes (No)
	0.125 - 0.150	3900 - 4400 (rest of the primaries)	Yes (No)
	0.150 - 0.175	4000 - 4400 (rest of the primaries)	Yes (No)
	0.175 - 0.200	4200 - 4400 (rest of the primaries)	Yes (No)
	0.200 - 0.225	4300 - 4400 (rest of the primaries)	Yes (No)
	0.225 - 1.1	All primaries	No
515	0.050 - 0.075	3400 - 4400 (rest of the primaries)	Yes (No)
	0.075 - 0.125	3500 - 4400 (rest of the primaries)	Yes (No)
	0.125 - 0.150	3600 - 4400 (rest of the primaries)	Yes (No)
	0.150 - 0.175	3700 - 4400 (rest of the primaries)	Yes (No)
	0.175 - 0.200	3800 - 4400 (rest of the primaries)	Yes (No)
	0.200 - 0.225	4000 - 4400 (rest of the primaries)	Yes (No)
	0.225 - 0.250	4200 - 4400 (rest of the primaries)	Yes (No)
	0.250 - 1.1	All primaries	No

**Table 3.** Different combination of number of primaries in a given range of cluster spread for streamer mode operations in single GEM. The values mentioned in the bracket "rest of the primaries" do not give rise to streamers in the corresponding range of the cluster spread.

percentage difference in operating voltages applied to the three GEM foils of a triple GEM detector. It may be noted that the general trend of the experimental data and numerical estimates matches qualitatively. In general, the numerical estimate is higher than the experimentally observed values for discharge probability.

From the figure, fast increase in discharge probability is observed in experiment [15] on either side of a minimum at  $\frac{\Delta V}{V} \sim -0.17$ , where the discharge probability is found to be less. The same minimum is reproduced in the simulated results although the magnitude of the estimated discharge probability is almost two orders of magnitude more than experimental value. It may be noted here that the simulation performed with equal voltages applied to three GEM foils in the voltage ranges, as mentioned in table 1, always leads to streamer formation in the third GEM foil. However, streamer formation is observed in both GEM2 and GEM3 when using an asymmetric distribution of voltages in the three GEM foils. Towards the negative values of  $(\frac{\Delta V}{V})$  from 0, the applied voltage

Applied Voltages $\Delta V_{\text{GEM}}$ (Volts)	Cluster Spread (mm)	Number of Primaries Range	Streamer Yes (No)
385	0.05 - 1.1	All Primaries	No
387	0.05 - 0.075	All primaries	Yes
	0.075 - 0.100	4200 - 4400 (rest of the primaries)	Yes (No)
	0.100 - 1.1	All Primaries	No
390	0.05 - 0.075	All primaries	Yes
	0.075 - 0.100	3500 - 4400 (rest of the primaries)	Yes (No)
	0.100 - 0.125	3800 - 4400 (rest of the primaries)	Yes (No)
	0.125 - 0.150	4000 - 4400 (rest of the primaries)	Yes (No)
	0.150 - 0.175	4100 - 4400 (rest of the primaries)	Yes (No)
	0.175 - 0.225	4200 - 4400 (rest of the primaries)	Yes (No)
	0.225 - 0.250	4300 - 4400 (rest of the primaries)	Yes (No)
	0.250 - 1.1	All primaries	Yes (No)
392	0.05 - 0.075	All primaries	Yes
	0.075 - 0.100	3300 - 4400 (rest of the primaries)	Yes (No)
	0.100 - 0.125	3400 - 4400 (rest of the primaries)	Yes (No)
	0.125 - 0.175	3600 - 4400 (rest of the primaries)	Yes (No)
	0.175 - 0.200	3700 - 4400 (rest of the primaries)	Yes (No)
	0.200 - 0.250	3800 - 4400 (rest of the primaries)	Yes (No)
	0.250 - 0.275	3900 - 4400 (rest of the primaries)	Yes (No)
	0.275 - 0.300	4000 - 4400 (rest of the primaries)	Yes (No)
	0.300 - 0.350	4100 - 4400 (rest of the primaries)	Yes (No)
	0.350 - 0.375	4200 - 4400 (rest of the primaries)	Yes (No)
	0.375 - 1.1	All primaries	Yes (No)

**Table 4.** Different combination of number of primaries in a given range of cluster spread for achieving streamer mode operations in Triple GEM for equal voltages applied to the three GEM foils. It may be noted here that, streamers have not been observed for the values mentioned in the bracket "rest of the primaries" corresponding to a certain range of cluster spread.

in GEM1 increased successively which enhanced the possibility for the formation of streamer in GEM2.

#### 4 Conclusion

A hybrid numerical model has been proposed to estimate response of single and multiple GEM-based ionization detectors. The generation of primaries has been computed using Monte-Carlo approach, while the transport and amplification of the charged species have been modelled using a hydrodynamic approach. Position and configuration of the seed cluster are found to have significant impact on the subsequent development of detector response. Energy resolution of single and triple GEM detectors for 5.9 keV photons from the  $^{55}\text{Fe}$  radiation has been estimated. The estimated values are found to be reasonably close to experimental values reported elsewhere. Finally, attempts have

been made to estimate discharge probabilities in such detectors when exposed to highly ionizing alpha radiation. Possibility of reducing discharge probability by applying asymmetric voltage distribution in multi-GEM structures has also been explored. The configuration and position of the primary seed have been found to have significant effect on the resulting probability of having either avalanche, or streamer mode operation. It has been possible to mimic the experimentally observed trends for this critically important factor, despite drastic simplifying assumptions.

The design goal of each experiment is different. Thus, finding an optimum point in ( $\frac{\Delta V}{V}$ ) for improvement in the discharge rates in an experiment can become a challenge as the discharge formation and propagation is a complex process that depend on tuning of other several performance parameters of the detector as well. The present numerical hybrid model may be of some help to predict the discharge rates in an experimental scenario utilizing an asymmetric configuration of operating voltages in a multistage GEM-based device with reasonable confidence.

## Acknowledgments

This work has been performed in the framework of RD51 collaboration. We wish to acknowledge the members of the RD51 collaboration for their help and suggestions. We would like to acknowledge necessary help and support from SINP. We would also like to thank the respective funding agencies, DAE and INO collaboration. Author P.Bhattacharya acknowledges the University Grant Commission and Dr. D.S.Kothari Post Doctoral Scheme for the necessary support.

## References

- [1] F. Sauli, *GEM: A new concept for electron amplification in gas detectors*, Nucl. Instrum. Meth. A 386 (1997) 531.
- [2] P. Abbon, et al., *The COMPASS experiment at CERN*, arXiv:hep-ex/0703049.
- [3] *LHCb Muon System Technical Design Report*, CERN LHCC 2001-010, LHCb TDR 4, 2001.
- [4] H.R. Schmidt, et al., *ALICE note*, 1999-56.
- [5] A. Colaleo et al., *CMS Technical Design Report for the Muon Endcap GEM Upgrade*, CERN-LHCC-2015-012 (2015).
- [6] M. Bozzo et al., *Design and Construction of the Triple GEM Detector for TOTEM*, Nuclear Science Symposium Conference Record, IEEE (2004) 447
- [7] M. G. Bagliesi et al., *The TOTEM T2 telescope based on triple-GEM chambers*, NIM A 617 (2010) 13
- [8] M. P. Titov, *New Developments and Future Perspectives of Gaseous Detectors*, Nucl. Instrum. Meth. A **581**, 25-37 (2007) [arXiv:0706.3516 [physics.ins-det]].
- [9] M. Abbas et al., *Triple-GEM discharge probability studies at CHARM: simulations and experimental results*, 2020 JINST15 P10013
- [10] G. Bencivenni, P. De Simone, F. Murtas, M. Poli-Lener, W. Bonivento, A. Cardini, C. Deplano, D. Pinci and D. Raspino, *Advances in triple-GEM detector operation for high-rate particle triggering*, Nucl. Instrum. Meth. A **513**, 264-268 (2003)
- [11] G. Bencivenni, P. De Simone, F. Murtas, M. Poli-Lener, W. Bonivento, A. Cardini, C. Deplano, D. Pinci and D. Raspino, *Performance of a triple-GEM detector for high rate charged particle triggering*, Nucl. Instrum. Meth. A **494**, 156-162 (2002)



- [12] G. Croci et al., *Discharge probability measurement of a Triple GEM detector irradiated with neutrons*, Nucl. Instrum. Meth. A **712**, (2013) 108
- [13] H. Raether, *Electron avalanches and breakdown in gases*, Butterworth, London (1964).
- [14] P. Gasik, et al., *Charge density as a driving factor of discharge formation in GEM-based detectors* Nucl. Instrum. Meth. A **870**, 116-122 (2017)
- [15] S. Bachmann, et al., *Discharge mechanisms and their prevention in the gas electron multiplier (GEM)*, Nucl. Instrum. Meth. A **479**, 294-308 (2002)
- [16] A. Bressan, M. Hoch, P. Pagano, L. Ropelewski, F. Sauli, S. Biagi, A. Buzulutskov, M. Gruwe, G. De Lentdecker and D. Mormann, *et al.*, *High rate behavior and discharge limits in micropattern detectors*, Nucl. Instrum. Meth. A **424**, 321-342 (1999)
- [17] C. Altunbas, M. Capéans, K. Dehmelt, J. Ehlers, J. Friedrich, I. Konorov, A. Gandi, S. Kappler, B. Ketzer and R. De Oliveira, *et al.*, *Construction, test and commissioning of the triple-GEM tracking detector for COMPASS*, Nucl. Instrum. Meth. A **490**, 177-203 (2002).
- [18] B. Ketzer, *Micropattern gaseous detectors in the COMPASS tracker*, Nucl. Instrum. Meth. A **494**, 142-147 (2002).
- [19] P. Bhattacharya, et al., *3D simulation of electron and ion transmission of GEM-based detectors*, Nucl. Instrum. Meth. A **870**, 64-72 (2017).
- [20] H. Natal Da Luz, P. Bhattacharya, L. A. S. Filho and L. E. F. M. França, *Ion backflow studies with a triple-GEM stack with increasing hole pitch*, JINST **13**, no.07, P07025 (2018)
- [21] M. Ball *et al.* [ALICE TPC], *Ion backflow studies for the ALICE TPC upgrade with GEMs*, JINST **9**, C04025 (2014).
- [22] Laurence E. Kline, John G. Siambis, *Computer Simulation of Electrical Breakdown in Gases; Avalanche and Streamer Formation*, Phys. Rev. A **5**, 794 (1972).
- [23] M. Jiang et.al, *3D PIC-MCC simulations of positive streamers in air gaps*, Phys. Plasmas **24**, 102112 (2017).
- [24] Jannis Teunissen, Ute Ebert, *Simulating streamer discharges in 3D with the parallel adaptive Afivo framework*, J. Phys. D: Appl. Phys. **50**, 474001 (2017).
- [25] D.D. Sentman, E.M. Wescott, *Red sprites and blue jets: thunderstorm-excited optical emissions in the stratosphere, mesosphere, and ionosphere*, Phys. Plasmas **2**, 2514 (1995).
- [26] P. K. Rout, J. Datta, P. Roy, P. Bhattacharya, S. Mukhopadhyay, N. Majumdar and S. Sarkar, *Fast simulation of avalanche and streamer in GEM detector using hydrodynamic approach*, JINST **16**, no.02, P02018 (2021).
- [27] P. Fonte, *Survey of physical modelling in Resistive Plate Chambers*, JINST **8** (2013) P11001.
- [28] [https://garfieldpp.web.cern.ch/garfieldpp/examples/avalanches\\_streamers/](https://garfieldpp.web.cern.ch/garfieldpp/examples/avalanches_streamers/).
- [29] Filippo Resnati, *Modelling of dynamic and transient behaviours of gaseous detectors*, RD-51 Open Lectures - 12/12/17 - CERN. <https://indico.cern.ch/event/676702/contributions/2769934/attachments/1574005/2484807/kjskjb.pdf>
- [30] S. Agostinelli *et al.* [GEANT4], *GEANT4—a simulation toolkit*, Nucl. Instrum. Meth. A **506**, 250-303 (2003). <https://geant4.web.cern.ch/>.
- [31] I.B. Smirnov, *Modeling of ionization produced by fast charged particles in gases*, Nucl. Instrum. Meth. A, **554** (2005) 474.

- [32] Jonathan Bortfeldt, *Development of Micro - Pattern Gaseous Detectors - Micromegas*, Diploma thesis. Online Pdf version at [http://www-static.etp.physik.uni-muenchen.de/dokumente/thesis/dipl\\_bortfeldt.pdf](http://www-static.etp.physik.uni-muenchen.de/dokumente/thesis/dipl_bortfeldt.pdf)
- [33] S.Y. Ha et al., *Energy resolution of a single GEM detector*, J. Korean Phys. Soc.55(2009) 2366.
- [34] R. N. Patra et al., *Measurement of basic characteristics and gain uniformity of a triple GEM detector*, Nucl. Instrum. Meth. A **862**, 25-30 (2017) [erratum: Nucl. Instrum. Meth. A **905**, 199 (2018)].
- [35] M. Gola et al., *Performance of the triple GEM detector built using commercially manufactured GEM foils in India*, Nucl. Instrum. Meth. A **951**, 162967 (2020)
- [36] P. Roy, et al., [arXiv:2004.13763 [physics.ins-det]].